Infrared Spectra of C_2H_6, C_2H_4, C_2H_2, and CO_2 Aerosols Potentially Formed in Titan's Atmosphere†

Chia C. Wang, Philipp Zielke, Ómar F. Sigurbjörnsson, C. Ricardo Viteri, and Ruth Signorell*

Department of Chemistry, University of British Columbia, 2036 Main Mall, Vancouver, BC V6T 1Z1, Canada

Received: May 3, 2009; Revised Manuscript Received: June 2, 2009

Pure and mixed aerosols of ethane, ethylene, acetylene and carbon dioxide were generated in a collisional cooling cell and characterized by Fourier transform infrared spectroscopy between 600 and 4000 cm^{-1}. Pure ethane, pure ethylene, and mixed ethane/ethylene initially form supercooled liquid droplets, which over time crystallize to their stable solid phases. These droplets are found to be long-lived (up to hours) for pure ethane and mixed ethane/ethylene, but short-lived (up to seconds) for pure ethylene. Acetylene and carbon dioxide form solid aerosol particles. Acetylene particles have a partially amorphous structure, while carbon dioxide particles are crystalline. The structure of the infrared bands of carbon dioxide is strongly determined by the particles' shape due to exciton coupling. The comparison of various mixed systems reveals that acetylene very efficiently induces heterogeneous crystallization. As reported earlier, the co-condensation of acetylene and carbon dioxide can lead to the formation of a metastable mixed crystalline phase. Our preliminary calculations show that this mixed phase has a monoclinic rather than the cubic structure proposed previously.

1. Introduction

Nitrogen and methane are the major components in Titan's atmosphere with mole fractions of 0.97 and 0.014 in the upper troposphere and lower stratosphere. In the upper atmosphere they lead to a rich photochemistry (refs 1−5 and references therein). Photochemical products include various hydrocarbons as well as nitrogen/carbon compounds with mole fractions that are for most species much less than 10^{-3}. By the formation of aerosols, these trace species have a significant influence on atmospheric processes on Titan. Compounds with low volatility contribute to the formation of the high-altitude aerosols by condensation, heterogeneous growth, and internal particle chemistry.[2,6−8] Species with higher volatility condense in lower regions of the atmosphere depending on the partial pressures and temperature.[1,4,9−12]

The present contribution studies the vibrational dynamics of aerosols formed from trace gases—ethane, acetylene, ethylene, and carbon dioxide—in Titan's atmosphere. The mole fractions of these compounds in Titan's stratosphere are 1.4×10^{-5}, 3.9×10^{-6}, 1.6×10^{-7}, and 1.6×10^{-8}, respectively.[2,3,13,14] Among those, ethane is assumed to be of crucial importance to Titan's troposphere. Strong evidence has been found for the formation of ethane clouds above the tropopause and in the troposphere in the polar regions.[10,15] Several studies also indicate that ethane aerosols might be important condensation nuclei for the formation of methane rain.[9,11,16] We have recently reported on the first infrared laboratory studies of methane and ethane aerosols.[17,18] From infrared spectra, we found evidence for the existence of supercooled ethane droplets under conditions prevalent in Titan's atmosphere. We determined their homogeneous as well as their heterogeneous crystallization dynamics. These studies are extended here to pure and mixed aerosols of ethane, ethylene, acetylene, and carbon dioxide. Our goal is to provide a first overview of the vibrational spectra of these aerosols and to search for characteristic infrared spectroscopic features that arise from phase changes, mixing, and particle properties such as the shape or the particle architecture.

2. Experimental Section

The aerosol particles were generated by bath gas cooling in our cooling cell and spectroscopically investigated *in situ* in the aerosol phase with rapid scan Fourier transform infrared spectroscopy between 600 and 4000 cm^{-1}. The experimental setup is described in more detail in refs 19−22. Briefly, the droplets or particles were formed by injection of a warm dilute sample gas into a cold bath gas (helium, Praxair 99.999%, pressure 900 mbar), which led to supersaturation and eventually to particle formation. The experiments were performed at a temperature of $T = 79$ K, which would corresponds to altitudes of 17 km and 62 km in Titan's atmosphere. Typical sample gas mixtures consisted of 0.25% to 0.5% substance in helium at a total pressure of 1050 mbar. C_2H_6 (99.994%), C_2H_4 (99.994%), C_2H_2 (99.6%), and CO_2 (99.998%) were purchased from Advanced Gas Technology or Praxair. C_2H_2 was purified by freezing out the stabilizer. While nitrogen would better mimic the conditions in Titan's atmosphere, we did these first experiments in helium bath gas to avoid possible cocondensation with nitrogen. The influence of nitrogen will be studied in forthcoming publications. The study of the different aerosols under conditions close to those in Titan's atmosphere has been the subject of a previous publication in the case of ethane[18] and will be the subject of forthcoming publications for the other substances. The goal of the present contribution is to elucidate the infrared spectroscopy of the different aerosols as a first crucial step.

The sample gases were introduced into the center of the cell through stainless steel tubes. The duration of the injections was controlled by Burkert solenoid magnetic valves. Typical injections times were 500−1000 ms. For the two-component particles (sections 3.2−3.4), we employed two different injection schemes.[23,24] Scheme 1: A premixed gas mixture consisting of

† Part of the special section "Chemistry: Titan Atmosphere".

* Author to whom correspondence should be addressed. Fax: +1 604 822-2847. E-mail: signorell@chem.ubc.ca.

10.1021/jp904106e CCC: $40.75
Published on Web 07/01/2009

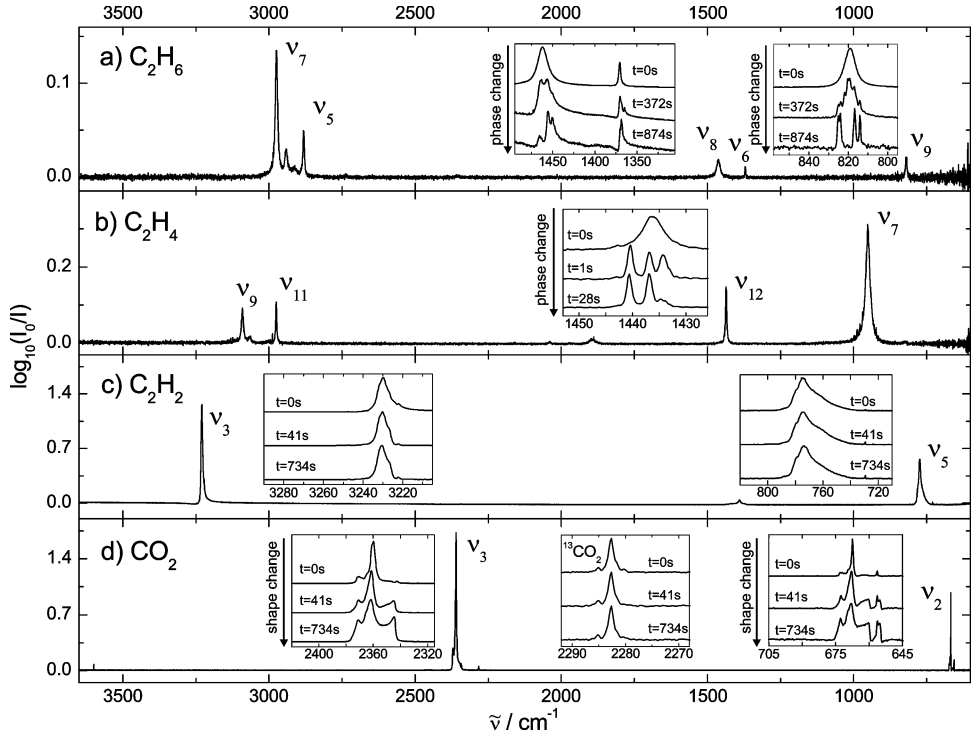

Figure 1. Infrared spectra of (a) pure ethane aerosol particles, (b) pure ethylene aerosol particles, (c) pure acetylene aerosol particles, and (d) pure carbon dioxide aerosol particles. The overview spectra were recorded immediately after particle formation ($t = 0$ s). The time-evolution of several bands is shown in the insets. $\tilde{\nu}$ is the wavenumber in cm^{-1}.

both substances diluted in helium was introduced into the cell. Scheme 2: The two different sample gases were introduced into the cell with a time delay of 500 ms between the end of the first and the beginning of the second injection. Under scheme 2, the first substance has already formed aerosols which act as condensation nuclei for the second substance.

3. Results and Discussion

3.1. Spectra of Pure Aerosols. Figures 1a to 1d show mid-infrared spectra of pure ethane, pure ethylene, pure acetylene, and pure carbon dioxide aerosols. All overview spectra were recorded immediately after injection of the gaseous samples ($t = 0$ s). The spectra in the insets show the time-evolution of some of the bands observed. For ethane, ethylene, and carbon dioxide these are the bands with the most pronounced time-dependence. As further explained below, the origin of the time-dependence for ethane and ethylene aerosols is a phase transition from supercooled liquid droplets to crystalline particles. The time-evolution of the spectra of carbon dioxide particles is caused by a change in the shape of the solid carbon dioxide particles. No pronounced time-dependence is observed for the acetylene particles under the present experimental conditions, which might be a consequence of a partially amorphous structure of these particles.

As we discussed in more detail in a recent contribution,[18] around 79 K ethane initially forms supercooled liquid droplets which are characterized by unstructured infrared bands (see trace a and insets at $t = 0$ s). As time passes ($t = 372$ s and $t = 874$ s), the droplets freeze as is evident from the time-dependence of the CH_3-deformation (ν_8 and ν_6) and the CH_3-rocking (ν_9) fundamental modes. The initially unstructured bands show more and more fine structure with increasing time due to the formation of an ordered phase. These modes are particularly sensitive to this phase transition, whereas the CH-stretching modes ν_7 and ν_5 are almost unaffected. From the analysis of the crystallization kinetics we deduced homogeneous volume freezing rate constants in the range of $J_v = 10^8$ cm^{-3} s^{-1}.[18] For a 1 μm particle, this translates into a freezing time of about 40 min. Supercooled ethane droplets have thus to be considered "long-lived" species and might therefore play a significant role in Titan's atmosphere. The stable crystal phase that results after the droplets are completely frozen ($t = 874$ s) corresponds to the bulk phase II.[25−27] A metastable intermediate phase (phase I)[25] often appears together with phase II at the beginning of the crystallization process, depending on the experimental conditions.[18] We have, however, never observed this phase to be stable under conditions relevant to Titan's atmosphere. The particles always convert rapidly into phase II, but this metastable phase might still play an important role in the initial condensation steps if ethane gas condenses onto other aerosol particles as discussed in ref 16.

If we compare the different substances discussed here, ethylene and ethane are closest to each other in terms of their phase transition data and the vapor pressures of the bulk liquid (boiling points, 170 and 185 K;[28] melting points, 104.00 and 90.36 K;[28] triple point temperatures, 103.99 K[29] and 90.34 K,[30] respectively). We thus expected a similar behavior of ethylene aerosols and ethane aerosols, which is confirmed by the formation of supercooled liquid ethylene droplets directly after gas injection (trace b and inset at $t = 0$ s), which crystallize over time ($t = 1$ s, and $t = 28$ s). However, in the case of ethylene the crystallization happens much faster than for ethane, i.e. within only a few seconds. Supercooled liquid ethylene droplets are thus only very "short-lived" species compared with supercooled ethane droplets. Similar to ethane, a metastable phase ("a-structure") develops at the beginning of the crystallization of ethylene particles before the stable $P2_1/n$ phase ("b-structure") at 79 K is formed.[31−34] This is illustrated in the inset in trace b for the CH_2-scissor vibration ν_{12}. The spectrum recorded at $t = 1$ s has similar contributions from the metastable

a-structure (part of the band at 1440 cm^{-1} and the band at 1434 cm^{-1}) as well as the stable b-structure" (part of the band at 1440 cm^{-1} and the band at 1437 cm^{-1}). At $t = 28$ s, the metastable structure has almost completely disappeared. Note that a similar behavior is also observed for the very weak rocking mode around 820 cm^{-1} and the overtone around 3050 cm^{-1}, which are, however, barely visible in trace b. All other vibrational bands are virtually unaffected by the phase transition. We used here the assignment of the bands to the a- and b-structure as it has been suggested for bulk phase infrared spectra.[32] Theses structures differ in the way the molecules are rotated around the C═C axis. In the b-structure, the two equivalent molecules are rotated in opposite directions by 27 degrees whereas in the a-structure the rotation has the same sense for the two molecules.[31] It has, however, never been verified whether the infrared spectral features are in agreement with the proposed structures a and b. To clarify this point, we have performed density functional calculations within the local density approximation with the ABINIT (version 4.6.5) program package,[35,36] using a plane-wave expansion of the electronic wave function. Core electrons were described by Toullier−Martins pseudopotentials. Phonon wavenumbers were calculated in the harmonic approximation. The monoclinic unit cell parameters for C_2H_4 (with two molecules per unit cell) were frozen at the experimental 85 K values,[31] while the total energy was minimized with respect to the atomic positions. The resulting minimum structure qualitatively reproduces the stable crystal structure (b-structure) found at 85 K.[31] The a-structure is obtained without any additional optimization by reversing the sense of rotation of the second molecule in the unit cell around its C═C bond. The accompanying change in energy is less than 1 kJ mol^{-1}. The calculated band splittings for the a-structure and the b-structure (11 cm^{-1} and 8 cm^{-1}, respectively) are qualitatively in agreement with the observed splittings in the infrared spectra (7 cm^{-1} and 5 cm^{-1}, respectively), although one has to keep in mind that these are rather delicate effects.

Acetylene immediately forms solid aerosol particles at 79 K (trace c), and no pronounced time-dependent features are observed (insets in trace c). The formation of solid particles is not so surprising because acetylene has a high sublimation point of 188 K (triple point temperature of 192 K).[28] Acetylene aerosols have previously been studied by Dunder and Miller.[37] Although ref 37 does not show the bending vibration ν_5 on an extended scale, our overall spectrum and the region of the CH-stretching mode ν_3 look very similar to the spectra by Dunder and Miller. They concluded that the aerosols are most likely formed in the high-temperature crystalline cubic phase ($Pa3$)[38] and do not transform to the low-temperature orthorhombic phase[38] (phase transition temperature is 133 K) in the time frame of the measurement, i.e. aerosol particles are frozen in the high temperature phase. Dunder and Miller ruled out amorphous or mixed crystalline structures for the particles they observed. Their conclusions, however, were not based on any modeling of the spectra. To elucidate the internal structure of our aerosol particles, we have performed vibrational exciton calculations[22,39−42,42] for the ν_5 band of particles with orthorhombic, cubic as well as partially amorphous structures. Since the ν_5 band has a strong molecular transition dipole it is sensitive to the phase of the particles. The comparison of the calculations with the experimental spectra shown in Figure 2 clearly speaks against crystalline particles. The band splittings of the crystalline phases are not observed in the experiment. The experimental spectrum is better reproduced by the spectrum of partially amorphous particles. Both show a broad band with little structure. In particular, there is a

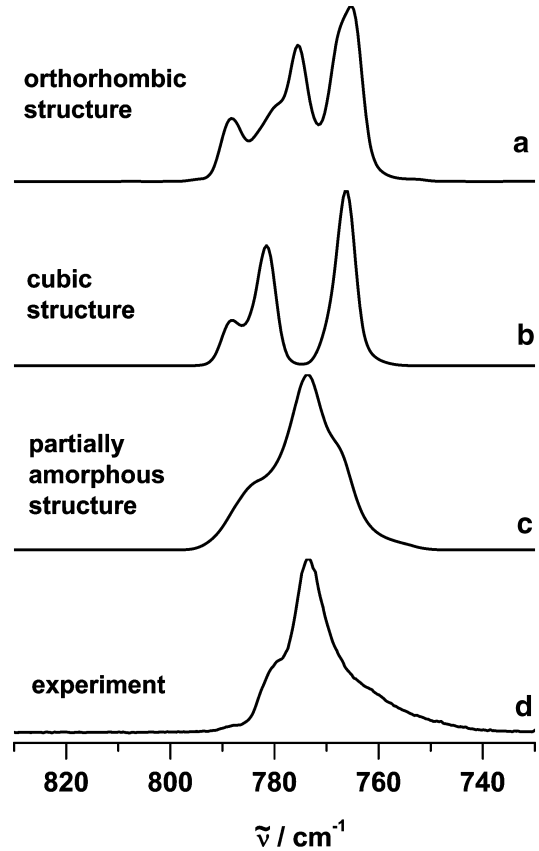

Figure 2. Vibrational exciton calculations for acetylene aerosol particles of different phases. (a) Orthorhombic crystal phase.[38] The calculation is for a parallelepiped with all edges of about equal length. (b) Cubic crystal structure.[38] The calculation is for a particle with a cubic shape. (c) Partially amorphous particle with a spherical shape. (d) Experimental infrared spectrum of acetylene aerosol (see Figure 1c).

characteristic shoulder on the high-frequency side. (Note that the agreement with the calculation for the partially amorphous particle is not expected to be perfect since we only rotated the molecules randomly by a maximum of 50 degrees without any optimization or annealing of the structure after rotation of the molecules.) The partially amorphous character also explains why the ν_5 band does not exhibit any pronounced time-dependent features. In our cooling cell, we often observe a change of aerosol particles over time from shapes with equal axis ratios to elongated particles[39,40,43−45] (see below, the behavior of CO_2 particles). Vibrational transitions with strong molecular transition dipoles, such as the ν_5 transition in acetylene (molecular transition dipole of about 0.23 D),[46] exhibit band structures which are very sensitive to the particles' shape if the particles have a crystalline structure. By contrast, amorphous particles tend to keep a spherical shape, and in addition, the shape sensitivity of infrared spectra of amorphous particles is much less pronounced.[40,44] Under the same conditions, under which the band structures of acetylene particles are stable (Figure 1c), we observe a pronounced change in the band structures of crystalline CO_2 particles with time (see Figure 1d and below), which is due to changes in the particles' shape.[39] By inference, the stability of the acetylene spectra with time is to be regarded as consistent with the assumption of partially amorphous particles.

Like acetylene aerosol particles, carbon dioxide particles are solid from the beginning (trace d in Figure 1; sublimation temperature of CO_2 is 195 K).[28] But in contrast to acetylene,

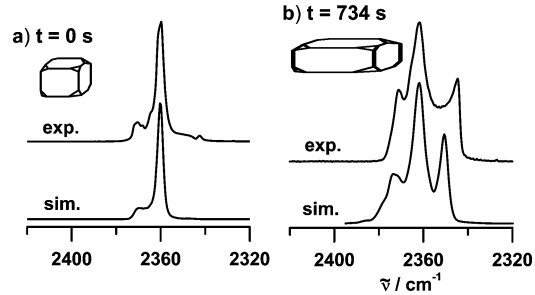

Figure 3. (a) Experimental infrared spectrum of CO_2 aerosols recorded at time $t = 0$ s (see also Figure 1d) together with a prediction from exciton calculations. (b) Experimental infrared spectrum of CO_2 aerosols recorded at time $t = 734$ s (see also Figure 1d) together with a prediction from exciton calculations (axis ration is about 1:1:3).

carbon dioxide immediately forms aerosol particles in the stable cubic phase,[47] as our and other groups have discussed and confirmed by calculations.[39,45,48,49] Therefore, the time evolution of the antisymmetric stretching mode ν_3 and the bending mode ν_2 of $^{12}CO_2$ (insets in trace d) is not the result of a phase change. Rather—as already mentioned above—it is caused by a change in the shape of the crystalline aerosol particles with time. The calculations in Figure 3, which are based on the molecular exciton model, show that particles are formed initially ($t = 0$ s) with an equal axis ratio (cuboctahedra). Over time, an increasing amount of elongated particles is developing, which gives rise to the characteristic spectral signatures found at $t = 734$ s. These calculations clearly reveal the strong molecular transition dipoles of the stretching and bending vibration (0.31 and 0.17 D, respectively) as the molecular origin of the shape sensitivity. For a more detailed discussion of such shape effects, we refer to our previous studies[39] and references therein. In contrast to the $^{12}CO_2$ bands, the $^{13}CO_2$ band around 2283 cm^{-1} does not show any time-dependence. The natural abundance of ^{13}C is only 1.1%. As a consequence this band does not exhibit strong exciton coupling and therefore no evolution due to changes of the particles' shape.[45]

3.2. Mixed C_2H_6−C_2H_4 Aerosols. For the understanding of atmospheric processes, it is important to know how the spectroscopic properties of pure aerosols and their crystallization behavior are modified by the presence of other substances which can either co-condense or act as condensation nuclei. As a first step, we report here on the properties of two-component systems with nearly equal content of both substances. Mixing ratios different from 1:1 will be the subject of forthcoming publications. To simulate possible cocondensation in the atmosphere, the aerosols are formed from premixed gas samples, while the sequential injection of the gases mimics the case when one type of aerosol acts as condensation nuclei for the second substance (see section 2).

The spectra of the mixed ethane/ethylene particles are depicted in Figure 4. The spectra on the left show the region of the ν_{12} band of ethylene, and those on the right show the region of the ν_9 band of ethane. As discussed above, both *pure* ethane and *pure* ethylene form supercooled liquid droplets immediately after the injection of the sample gas. Furthermore, we found ethane droplets to be long-lived (up to hours) and ethylene droplets to be short-lived species (up to seconds). It is therefore not surprising that injection of a premixed gas sample of ethane and ethylene also leads to the formation of supercooled droplets (Figure 4a). What is more surprising is the fact that the very fast crystallization observed for pure ethylene particles is strongly inhibited by the presence of ethane. This can only be understood by the formation of mixed supercooled droplets.

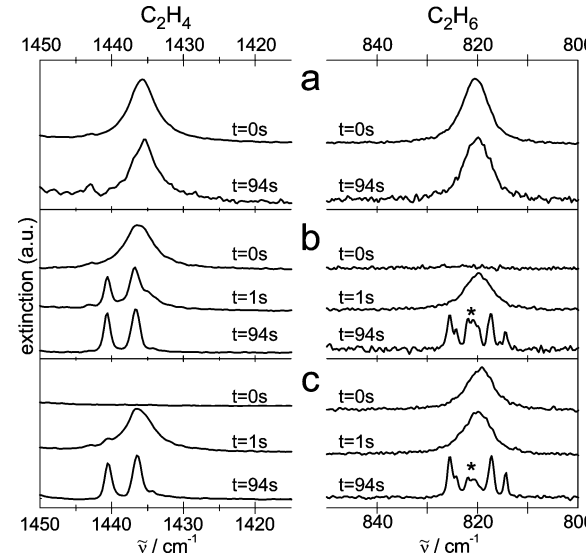

Figure 4. Time-evolution of experimental infrared spectra of mixed ethylene/ethane aerosols in the region of the ν_{12} band of ethylene and the ν_9 band of ethane. (a) Injection of a premixed gas sample. (b) Sequential injection of ethylene gas (first) and ethane gas (second). (c) Sequential injection of ethane gas (first) and ethylene gas (second). Asterisks mark intermediate absorptions due to the unstable phase I of C_2H_6.

Mixing leads to freezing point depression in the mixture, which in turn leads to a lower crystallization rate. While pure ethylene particles are already crystalline after 1 s (see Figure 1b), the mixed particles are still liquid droplets after 94 s (see Figure 4a). The ethylene band shows the first signs of crystallization only after several hundred seconds (not shown here). It is at the same time that the ethane bands also start to show the first signs of crystallization. In other words, the liquid mixture crystallizes on a similar time scale as the pure ethane droplets (Figure 1a). Furthermore, after crystallization of the mixed droplets is complete, most spectral features of ethylene and ethane are essentially the same as those of the pure crystalline substances, a hint that no mixed crystal phase is formed. (Slight deviations are found for the ν_7 band of ethylene, which might be due to exciton coupling.) Since the crystalline particles are formed from a liquid mixture they are likely to consist of a coarse grain structure with separate regions of pure ethylene and pure ethane.

Figures 4b and 4c illustrate what happens if the two gases are injected into the cell sequentially with a time delay (see section 2). Before the second substance is injected, the first substance shows the characteristic unstructured bands of liquid droplets ($t = 0$ s trace b left and trace c right, respectively). The time delay between the injection of the first and the second substance was chosen so that the second substance can form a shell around the already present droplet/particle of the first substance. At the very first moment after injection of the second substance, this coating is liquid ($t = 1$ s trace b right and trace c left, respectively). However, the contact of the two substances immediately initiates and strongly accelerates (compared with pure particles) the crystallization both of the core and of the liquid shell ($t = 1$ s and $t = 94$ s). Since crystallization is heterogeneous in this case the crystallization of core and shell is faster than the crystallization of the pure droplets (Figures 1a and 1b). For these core−shell architectures (Figures 4b and 4c), it does not matter for the crystallization dynamics whether a certain substance forms the shell or the core. The dynamics is essentially the same because the contact surface between the

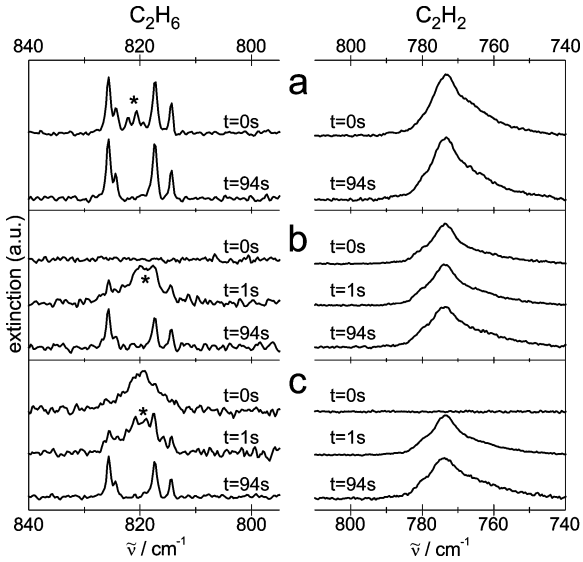

Figure 5. Time-evolution of experimental infrared spectra of mixed ethane/acetylene aerosols in the region of the ν_9 band of ethane and the ν_5 band of acetylene. (a) Injection of a premixed gas sample. (b) Sequential injection of acetylene gas (first) and ethane gas (second). (c) Sequential injection of ethane gas (first) and acetylene gas (second). Asterisks mark intermediate absorptions due to the unstable phase I of C_2H_6.

two substances is the same. The asterisks in Figure 4 label contributions from the metastable phase of ethane mentioned in section 3.1.[18]

3.3. Mixed $C_2H_6-C_2H_2$ and $C_2H_4-C_2H_2$ Aerosols. Figure 5 shows the spectra of mixed ethane/acetylene aerosols. The aerosol spectra for premixed gas samples (panel a) resemble a superposition of spectra of pure crystalline ethane aerosols (Figure 1a) and pure acetylene aerosols in (Figure 1c). We found two minor spectral differences compared with pure particles. The acetylene band of the mixture at $t = 0$ s does not show the weak shoulder observed at 780 cm^{-1} for pure acetylene (Figure 1c and Figure 2). Moreover, the intensity ratio of the doublet at 825 cm^{-1} is different in the mixture ($t = 94$ s in Figure 5a left) compared with the spectrum of pure ethane particles at $t = 874$ s in Figure 1a. Since we observed a similar variation of this intensity ratio also for *pure* ethane aerosols formed under different conditions, this feature cannot be taken as a characteristic for the mixtures. The major effect of mixing is the immediate crystallization of ethane. We no longer observe any liquid ethane phase within the time resolution of the experiment, in contrast to what we saw for pure ethane aerosols (Figure 1a) and for mixed ethane/ethylene aerosols (Figure 4a). It is thus clear that the presence of acetylene leads to the immediate crystallization of ethane. This behavior and the similarity of the spectral features with pure aerosols are strong indications that ethane and acetylene do not form stable homogeneously mixed (on a molecular level) particles. Instead, the two substances are likely to form domains of pure components. The faster crystallization of ethane in the mixture compared with pure ethane is thus a consequence of heterogeneous crystallization. Two different types of domain formation are conceivable: the formation of an acetylene core with an ethane shell or the formation of regions of pure ethane and pure acetylene within a single aerosol particle. Core−shell particles can form from premixed gas samples if one substance condenses at a much higher temperature than the other during the cooling process. However, under our experimental conditions, acetylene is expected to condense (as a solid) at a temperature that is only a few degrees higher than the temperature at which ethane starts to condense (as a liquid). We believe that this makes the core−shell formation a rather unlikely scenario. More likely seems the formation of particles with separate regions of pure ethane and pure acetylene. In this case, ethane and acetylene might initially condense into an unstable homogeneous mixture, which, however, would separate quickly into pure regions.

Acetylene−ethane core−shell particles are formed if acetylene gas is introduced prior to ethane gas (see Figure 5b). In the very first moments ($t = 1$ s in panel b), the ethane shell shows a broad band with some structure on both sides. The side bands are the signatures of the particles in the ensemble that are already in the stable crystal phase II at that same time. The broad band is the contribution from particles which are still in the metastable phase I. The ethane shell is converted completely into the stable crystal phase II after only $t = 9$ s (not shown). The crystallization is thus not only much faster than the crystallization of pure ethane particles (Figure 1a) but also faster than the crystallization of ethylene−ethane core−shell particles (Figure 4b). The ethylene−ethane core−shell particles still show contributions from the intermediate phase around 820 cm^{-1} at $t = 94$ s, which is not the case for the acetylene−ethane core−shell particles at $t = 94$ s. Acetylene thus seems to be more efficient than ethylene to initiate the heterogeneous crystallization of ethane. The acetylene bands in the acetylene−ethane core−shell particles (Figure 5b right) have the same band structure as pure acetylene particles (Figures 1c and 2). Furthermore, they do not show any pronounced time dependence under the present experimental conditions, i.e. the solid acetylene core is not influenced by the crystallization of the ethane shell.

The same results are found in the reverse case, i.e. an ethane core with an acetylene shell in Figure 5c. The ethane core crystallizes on the same time scale as the ethane shell does in panel b. This is to be expected because the contact area with acetylene is the same. Again, the time scale for the crystallization of the ethane−acetylene core−shell particles is faster than the time scale for the ethane−ethylene core−shell architecture in Figure 4c. The acetylene bands in Figure 5c on the right are again time-independent, indicating that the acetylene shell is not influenced by the crystallization of the ethane core.

The trends observed for the ethylene/acetylene mixtures in Figure 6 are identical to those for the ethane/acetylene mixtures described above. Acetylene leads to an immediate and complete crystallization of ethylene to the stable phase both for the injection of premixed gas samples (panel a) and for the sequential injections (panels b and c). In all cases, the crystallization of ethylene is faster than for pure ethylene (Figure 1b) or mixed ethylene/ethane aerosols (Figure 4). Similarly, acetylene is found to be more efficient than ethane to initiate the heterogeneous crystallization of ethylene. The features in the acetylene bands for the ethylene/acetylene mixtures are also equivalent to those observed for the ethane/acetylene mixtures. For the core−shell particles (panels b and c) they are the same as for the pure acetylene particles (Figure 1c) with acetylene indifferent to the crystallization of ethylene. The band shapes in the premixed case (panel a) look slightly different. Just as in the case of premixed ethane/acetylene particles at $t = 0$ s, the weak shoulder at 780 cm^{-1} (Figures 1c and 2) is absent. In addition, the low frequency tail is more pronounced compared with pure particles. We believe that particles formed from these premixed gas samples consist of separate regions of pure ethylene and pure acetylene. The argument is again the condensation temperature, quite analogous to the case of ethane/acetylene (see above). A second hint comes from the slightly

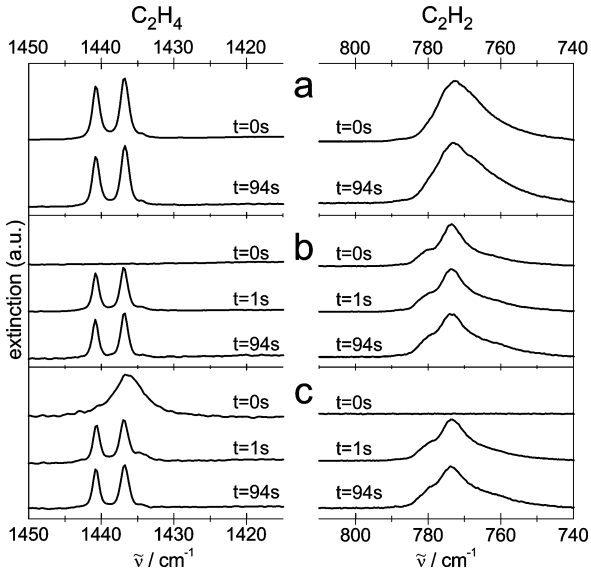

Figure 6. Time-evolution of experimental infrared spectra of mixed ethylene/acetylene aerosols in the region of the ν_{12} band of ethylene and the ν_5 band of acetylene. (a) Injection of a premixed gas sample. (b) Sequential injection of acetylene gas (first) and ethylene gas (second). (c) Sequential injection of ethylene gas (first) and acetylene gas (second).

different acetylene band structure in Figure 6a compared with Figures 6b and 6c (and Figure 1c). This difference might be a consequence of the different particle architecture, i.e. particles with pure ethylene regions and pure acetylene regions versus core−shell particles. The less structured acetylene bands in the first case might be a consequence of a more amorphous structure of acetylene forming near the large interface between regions of pure acetylene and pure ethylene. For a core−shell architecture this effect would be less pronounced because of the much smaller interface region, which explains why the signatures of the core−shell particles are essentially the same as those of the pure particles.

Acetylene makes the heterogeneous crystallization of ethane and ethylene more efficient (Figures 5 and 6, respectively) compared with the ethane/ethylene mixtures (Figure 4). Many factors can be responsible for this behavior, such as miscibility, structure, and heat of condensation. From the limited number of data we have so far, it is not possible to disentangle the different contributions. However, by replacing acetylene with carbon dioxide we can at least get an impression on how sensitively crystallization depends on the type of substances. We expected the crystallization behavior of ethane in ethane/carbon dioxide mixtures to be very similar to ethane/acetylene mixtures (Figure 5). We found, however, that ethane crystallization in ethane/carbon dioxide mixtures shows a behavior that lies in between ethane/etylene mixtures (Figure 4) and ethane/acetylene mixtures (Figure 5). Apparently, the heterogeneous crystallization is very sensitive to the type of substances involved.

3.4. Mixed $C_2H_2-CO_2$ Aerosols. As outlined in section 3.1, pure acetylene and pure carbon dioxide particles do not show any phase transitions after particle formation (see Figures 1c and 1d). Both substances immediately form solid particles. This behavior is consistent with their high-lying sublimation points (188 and 195 K, respectively).[28] Carbon dioxide forms crystalline particles, while acetylene particles are probably in a partially amorphous state according to the arguments given in section 3.1. The sequential injection of the two gases is thus expected to produce core−shell particles for which the phase of the core and that of the shell are similar to those of the pure particles. Figure 7 confirms this expectation. Panel a shows the ν_3 and the ν_5 band of acetylene (left) together with the ν_3 bands of $^{12}CO_2$ and of $^{13}CO_2$ for particles with a carbon dioxide core and an acetylene shell. (Note that $^{13}CO_2$ is present in its natural

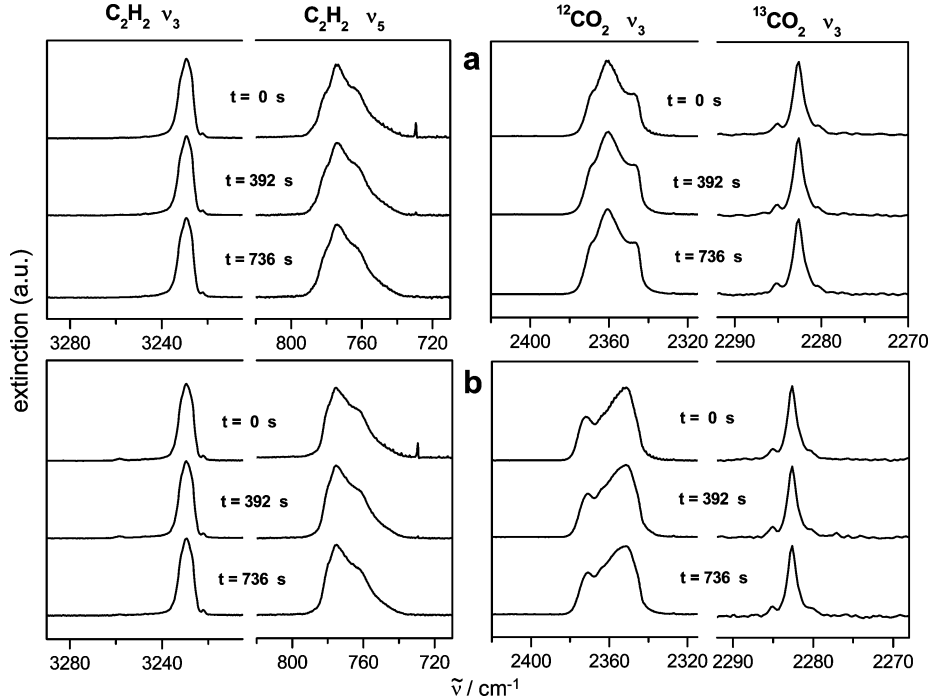

Figure 7. Time-evolution of experimental infrared spectra of mixed acetylene/carbon dioxide aerosols. (a) Sequential injection of carbon dioxide gas (first) and acetylene gas (second). (b) Sequential injection of acetylene gas (first) and carbon dioxide gas (second). The weak sharp modulations of some bands arise from residual C_2H_6 or CO_2 gas. Note that $t = 0$ s is here the time just after injection of the second substance. This is in contrast to panels b and c in Figures 4, 5, and 6, for which $t = 0$ s is the time just after injection of the first substance.

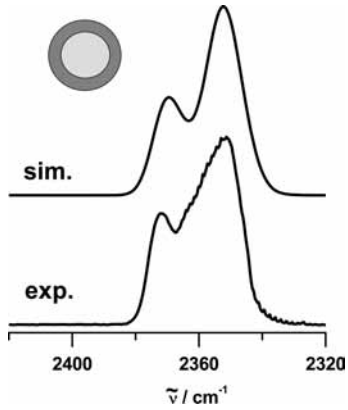

Figure 8. Vibrational exciton calculations (upper trace) for a carbon dioxide shell together with the experimental spectrum of a carbon dioxide shell (lower trace and Figure 7b).[38]

abundance of 1.1%.) In this case, the coating with acetylene was performed after the CO_2 cores have turned into mostly elongated shapes (see $t = 41$ s and $t = 734$ s in Figure 1d for comparison). As expected, the spectral features of the core and of the shell look similar to those of the pure particles (Figures 1c and 1d). The acetylene bands are consistent with partially amorphous particles. It is therefore not astonishing that the acetylene bands do not show pronounced time-dependence (Figure 7a and section 3.1). The $^{12}CO_2$ band exhibits the features of elongated crystalline particles (Figures 1d and 3). In contrast to pure particles (Figure 1d), however, it does not show a pronounced time-dependence under these experimental conditions. The acetylene coating obviously prevents further change of the shape of the carbon dioxide core.

A very similar behavior is found for core−shell particles with acetylene in the core and carbon dioxide in the shell (Figure 7b). The C_2H_2 core again shows similar spectral features as the pure C_2H_2 particles (Figure 1c). The same is true for the $^{13}CO_2$ band. Only the ν_3 band of $^{12}CO_2$ band significantly differs from the pure spectra (Figure 1d) as well as from the spectra with carbon dioxide in the core and acetylene in the shell (Figure 7a). As explained in section 3.1 (see also refs 39, 45, 48, 49), this band is very sensitive to the shape of the particles as a consequence of strong exciton coupling. In the case of these core−shell particles, the shell is the shape which determines the exciton coupling pattern and thus the band shape. As we have demonstrated previously,[22,24,44] the spectrum of a CO_2 shell is characterized by two bands at about 2371 and 2352 cm^{-1}, which is exactly the feature of the ν_3 band of $^{12}CO_2$ found in Figure 7b. Figure 8 shows the ν_3 band of panel b together with an corresponding exciton calculation for a CO_2 shell. It is noteworthy that the shape of the antisymmetric stretching band of $^{13}CO_2$ is not influenced by exciton coupling and hence it is not affected by the shell architecture. With a natural abundance of only 1.1%, the distance between $^{13}CO_2$ molecules is simply too large for any appreciable coupling.

Gough et al. have earlier reported that the co-condensation of acetylene gas and carbon dioxide gas can lead to the formation of a metastable (with respect to the pure phases) mixed crystal phase.[50,51] The formation of this phase was observed over a limited range of mole fractions with a maximum around 0.5. It was concluded that the stoichiometric ratio is 1:1 and that the mixed phase is a cubic crystal phase. Figure 9 demonstrates that such a mixed crystal phase is also formed in aerosol particles if a premixed C_2H_2/CO_2 gas mixture is rapidly injected into our cooling cell. The ν_3 band of acetylene and the ν_3 band of $^{13}CO_2$ are perfect indicators for the formation of this mixed crystal phase. The ν_3 band of acetylene shifts to higher energy by about 30 cm^{-1} from 3229 cm^{-1} in pure C_2H_2 to 3259 cm^{-1} in the mixed crystal phase. The ν_3 band of $^{13}CO_2$ shifts to lower energy by about 5 cm^{-1} from 2282 cm^{-1} in pure CO_2 to 2277 cm^{-1} in the mixed crystal phase. Since the acetylene fraction of our gas mixture contains more C_2H_2 than CO_2 (ratio 1.5), we find immediately after particle formation ($t = 0$ s) all $^{13}CO_2$ bound in the mixed phase (no band at 2282 cm^{-1}), while there are signatures of acetylene bound in the mixed phase (3259 cm^{-1}) as well as signatures of pure acetylene (3229 cm^{-1}). Over time, the metabstable mixed phase decomposes into the more stable pure phases as confirmed by the time evolution ($t = 392$ s and $t = 736$ s) in Figure 9.

Currently, theoretical investigations are under way in our research group to clarify the nature of the mixed crystal phase. We have performed density functional calculations within the local density approximation with the ABINIT (version 4.6.5) program package[35,36] (see section 3.1). The goal was to find out whether the original assumption of a cubic phase[50] is a plausible explanation or whether another phase is more realistic. Furthermore, we were interested in determining the spectral features of this mixed phase. We started from the cubic CO_2 unit cell[47] with two of the CO_2 molecules replaced by C_2H_2. Minimizing the total energy with respect to atomic positions with the unit cell constrained to remain cubic yields an energy of 8.3 kJ mol^{-1} above the most stable separate phases (cubic CO_2, orthorhombic C_2H_2). This structure, however, is only

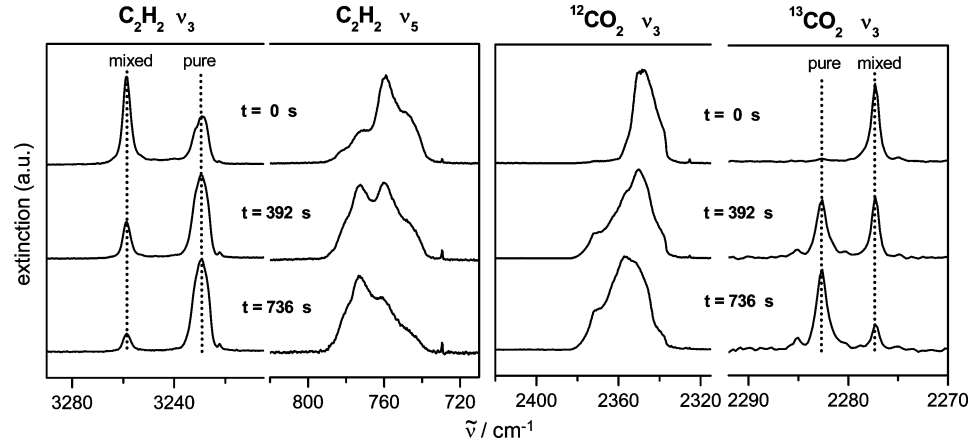

Figure 9. Time-evolution of experimental infrared spectra of mixed acetylene/carbon dioxide aerosols that were formed by injection of a premixed gas sample of acetylene and carbon dioxide.

metastable with respect to symmetry breaking as indicated by very low-frequency lattice modes. Unconstrained minimization of the energy produces a monoclinic unit cell with a β angle of 65 degrees and an energy of only 1.4 kJ above the demixed pure phases. The calculations thus clearly favor a monoclinic over the cubic mixed structure proposed by Gough et al.[50,51] We have also determined the shift of the ν_3 band of acetylene between the mixed monoclinic crystal and the pure acetylene crystal. The calculated shift is 15 cm^{-1} toward higher wavenumbers relative to the cubic C_2H_2 and 79 cm^{-1} relative to orthorhombic C_2H_2. In our case, pure acetylene is neither cubic nor orthorhombic but partially amorphous, for which we expect a shift in the same range. Both the sign and the order of magnitude of the shift is in agreement with the experimental shift of 30 cm^{-1}.

Other interesting questions relate to the decomposition process of the mixed phase and to the architecture of the resulting demixed particles. Again, plausible scenarios are the formation of aerosol particles with separate regions of pure acetylene and pure carbon dioxide as well as the formation of core−shell type particles. Information on such particle architectures is in principle contained in vibrational bands with strong exciton coupling, i.e. the ν_3 band of $^{12}CO_2$ and the ν_5 band of acetylene. As explained in previous sections, exciton coupling makes these bands not only sensitive to the phase but also to the architecture. Consequently, these two bands do not only exhibit a simple shift (Figure 9) in going from pure to mixed phases, but the band structure changes as well. A more complete analysis will be the subject of a forthcoming publication.

4. Summary

The present contribution provides an overview of the properties of pure and mixed aerosol particles of ethane, ethylene, acetylene, and carbon dioxide. The particles were generated in a collisional cooling cell at a temperature of 79 K (corresponding to altitudes of 17 km and 62 km in Titan's atmosphere) and investigated with mid-infrared spectroscopy. Two different types of mixed particles were studied: Aerosols formed from premixed gas samples simulate co-condensation in a planetary atmosphere, while sequential injection of gases mimics the situation where one type of aerosol particles serves as condensation nuclei for a second substance.

Pure ethane and pure ethylene initially form supercooled liquid droplets, which crystallize to the stable bulk phase over time. While the crystallization of ethane is slow (up to hours,),[18] ethylene crystallizes very quickly (seconds). By contrast, pure acetylene forms solid aerosol particles with a partially amorphous structure, which do not convert to the stable orthorhombic crystal phase on the time scale of our experiment. Carbon dioxide also forms solid particles from the beginning, which are crystalline in the stable cubic phase. The infrared spectra of these particles feature band structures that are determined by the shape of the aerosol particles as a consequence of the pronounced vibrational exciton coupling.

Co-condensation of two different substances leads in only two cases to the formation of homogeneously mixed (on a molecular level) droplets/particles: The injection of a premixed gas sample of either ethane and ethylene or acetylene and carbon dioxide. The former produces homogeneous liquid droplets, which are stabilized against crystallization. Therefore, crystallization happens only slowly (up to hours), so that supercooled mixed ethane/ethylene droplets as well as supercooled pure ethane droplets must be considered long-lived species with possibly important implications for cloud processes on Titan. The homogeneous particles observed following the cocondensation of acetylene and carbon dioxide are in agreement with earlier reports[50] of a mixed metastable crystal phase. We find evidence that this phase has a monoclinic structure rather than the cubic structure proposed earlier. In all other cases, co-condensation does not lead to the formation of homogeneously mixed phases. The experimental results hint that these particles consist of coarse grained structures of domains of pure substances.

The sequential injection of two gases allowed us to compare the heterogeneous crystallization of ethane and ethylene with the homogeneous crystallization of pure droplets described above. We find that while heterogeneous crystallization is always much faster (less than minutes), the crystallization dynamics sensitively depends on the type of substance. Acetylene was found particularly efficient to induce crystallization through contact with another substance.

Acknowledgment. This project was financially supported by the Natural Sciences and Engineering Research Council of Canada, the Canada Foundation for Innovation, the A. P. Sloan Foundation (R.S.), and the German Research Foundation DFG (P.Z.). Allocation of CPU-time on WestGrid facilities is gratefully acknowledged.

References and Notes

(1) Atreya, S. K.; Adams, E. Y.; Niemann, H. B.; Demick-Montelara, J. E.; Owen, T. C.; Fulchignoni, M.; Ferri, F.; Wilson, E. H. *Planet. Space Sci.* **2006**, *54*, 1177–1187.

(2) Waite, J. H., Jr; Young, D. T.; Cravens, T. E.; Coates, A. J.; Crary, F. J.; Magee, B.; Westlake, J. *Science* **2007**, *316*, 870–875.

(3) Coustenis, A.; et al. *Icarus* **2007**, *189*, 35−62.

(4) Lunine, J. I.; Atreya, S. K. *Nat. Geosci.* **2008**, *1*, 159–164.

(5) Krasnopolsky, V. A. *Icarus* **2009**, *201*, 226–256.

(6) McKay, C. P.; Coustenis, A.; Samuelson, R. E.; Lemmon, M. T.; Lorenz, R. D.; Cabane, M.; Rannou, P.; Drossart, P. *Planet. Space Sci.* **2001**, *49*, 79–99.

(7) Israël, G.; et al. *Nature* **2005**, *438*, 796–799.

(8) Liang, M.-C.; Yung, Y. L.; Shemansky, D. E. *Astrophys. J.* **2007**, *661*, L199–L202.

(9) Graves, S. D. B.; McKay, C. P.; Griffith, C. A.; Ferri, F.; Fulchignoni, M. *Planet. Space Sci.* **2008**, *56*, 346–357.

(10) Griffith, C. A.; Penteado, P.; Rannou, P.; Brown, R.; Boudon, V.; Baines, K. H.; Clark, R.; Drossart, P.; Buratti, B.; Nicholson, P.; McKay, C. P.; Coustenis, A.; Negrao, A.; Jaumann, R. *Science* **2006**, *313*, 1620–1622.

(11) Barth, E. L.; Toon, O. B. *Icarus* **2006**, *182*, 230–250.

(12) Lorenz, R. D.; Lunine, J. I. *Icarus* **2002**, *158*, 557–559.

(13) Vinatier, S.; Bézard, B.; Fouchet, T.; Teanby, N. A.; de Kok, R.; Irwin, P. G. J.; Conrath, B. J.; Nixon, C. A.; Romani, P. N.; Flasar, F. M.; Coustenis, A. *Icarus* **2007**, *188*, 120–138.

(14) Teanby, N. A.; Irwin, P. G. J.; de Kok, R.; Nixon, C. A.; Coustenis, A.; Royer, E.; Calcutt, S. B.; Bowles, N. E.; Fletcher, L.; Howett, C.; Taylor, F. W. *Icarus* **2008**, *193*, 595–611.

(15) Rannou, P.; Montmessin, F.; Hourdin, F.; Lebonnois, S. *Science* **2006**, *311*, 201–205.

(16) Curtis, D. B.; Hatch, C. D.; Hasenkopf, C. A.; Toon, O. B.; Tolbert, M. A.; McKay, C. P.; Khare, B. N. *Icarus* **2008**, *195*, 792–801.

(17) Signorell, R.; Jetzki, M. *Phys. Rev. Lett.* **2007**, *98*, 013401.

(18) Sigurbjörnsson, Ó. F.; Signorell, R. *Phys. Chem. Chem. Phys.* **2008**, *10*, 6211–6214.

(19) Kunzmann, M. K.; Signorell, R.; Taraschewski, M.; Bauerecker, S. *Phys. Chem. Chem. Phys.* **2001**, *3*, 3742–3749.

(20) Signorell, R. *Mol. Phys.* **2003**, *101*, 3385–3399.

(21) Jetzki, M. Doctoral Thesis; Cuvillier Verlag: Göttingen, 2005.

(22) Firanescu, G.; Hermsdorf, D.; Ueberschaer, R.; Signorell, R. *Phys. Chem. Chem. Phys.* **2006**, *8*, 4149–4165.

(23) Kunzmann, M. K. Doctoral Thesis; Cuvillier Verlag: Göttingen, 2002.

(24) Signorell, R.; Jetzki, M.; Kunzmann, M.; Ueberschaer, R. *J. Phys. Chem. A* **2006**, *110*, 2890–2897.

(25) van Nes, G. J. H.; Vos, A. *Acta Crystallogr. B* **1978**, *34*, 1947–1956.

(26) Wisnosky, M. G.; Eggers, D. F.; Frederickson, L. R.; Decius, J. C. *J. Chem. Phys.* **1983**, *79*, 3505–3512.

(27) Rest, A. J.; Warren, R.; Murray, S. C. *Appl. Spectrosc.* **1996**, *50*, 517–520.
(28) *CRC Handbook of Chemistry and Physics*, 84th ed.; Lide, D. R., Ed.; CRC Press: Boca Raton, FL, 2004.
(29) Jahangiri, M.; Jacobsen, R. T.; Steward, R. B.; McCarty, R. D. *J. Phys. Chem. Ref. Data* **1986**, *15*, 593–734.
(30) Younglove, B. A.; Ely, J. F. *J. Phys. Chem, Ref. Data* **1987**, *16*, 577–798.
(31) van Nes, G. J. H.; Vos, A. *Acta Crystallogr. B* **1979**, *35*, 2593–2601.
(32) Jacox, M. E. *J. Chem. Phys.* **1962**, *36*, 140–143.
(33) Rytter, E.; Gruen, D. M. *Spectrochim. Acta A* **1979**, *35*, 199–207.
(34) Wieder, G. M.; Dows, D. A. *J. Chem. Phys.* **1962**, *37*, 2990–2995.
(35) Gonze, X.; et al. *Comput. Mater. Sci.* **2002**, *25*, 478–492.
(36) The ABINIT code is a common project of the Universite Cathilique de Louvain, Corning Incorporated, and other contributors (URL http://www.abinit.org).
(37) Dunder, T.; Miller, R. E. *J. Chem. Phys.* **1990**, *93*, 3693–3703.
(38) McMullan, R. K.; Kvick, Å.; Popelier, P. *Acta Crystallogr. B* **1992**, *48*, 726–731.
(39) Sigurbjörnsson, Ó. F.; Firanescu, G.; Signorell, R. *Annu. Rev. Phys. Chem.* **2009**, *60*, 127–146.
(40) Firanescu, G.; Signorell, R. *J. Phys. Chem. B* **2009**, *113*, 6366–6377.
(41) Firanescu, G.; Luckhaus, D.; Signorell, R. *J. Chem. Phys.* **2006**, *125*, 144501.
(42) Signorell, R. *J. Chem. Phys.* **2003**, *118*, 2707–2715.
(43) Sigurbjörnsson, Ó. F.; Firanescu, G.; Signorell, R. *Phys. Chem. Chem. Phys.* **2009**, *11*, 187–194.
(44) Signorell, R.; Jetzki, M. *Faraday Discuss.* **2008**, *137*, 51–64.
(45) Signorell, R.; Kunzmann, M. K. *Chem. Phys. Lett.* **2003**, *371*, 260–266.
(46) Smit, W. M. A.; Van Straten, A. J.; Visser, T. *J. Mol. Struct.* **1978**, *48*, 177–189.
(47) Wyckoff, R. W. G. *Crystal Structures*; John Wiley and Sons; New York, London, 1963; Vol. 1.
(48) Gough, T. E.; Wang, T. *J. Chem. Phys.* **1996**, *105*, 4899–4904.
(49) Disselkamp, R.; Ewing, G. E. *J. Chem. Phys.* **1993**, *99*, 2439–2448.
(50) Gough, T. E.; Rowat, T. E. *J. Chem. Phys.* **1998**, *109*, 6809–6813.
(51) Gough, T. E.; Wang, T. *J. Chem. Phys.* **1995**, *102*, 3932–3937.

JP904106E